Stem Cell Reports
Article

ISSCR

OPEN ACCESS

BMAL1 Deficiency Contributes to Mandibular Dysplasia by Upregulating MMP3

Jiajia Zhao,[1,5] Xin Zhou,[1,5] Qingming Tang,[1,5] Ran Yu,[1] Shaoling Yu,[1] Yanlin Long,[1] Cen Cao,[1] Jun Han,[1] Anbing Shi,[2] Jeremy J. Mao,[3] Xiong Chen,[4] and Lili Chen[1,*]

[1]Department of Stomatology, Union Hospital, Tongji Medical College, Huazhong University of Science and Technology, Wuhan 430022, China
[2]Department of Biochemistry and Molecular Biology, School of Basic Medicine and the Collaborative Innovation Center for Brain Science, Tongji Medical College, Huazhong University of Science and Technology, Wuhan 430030, China
[3]Center for Craniofacial Regeneration, College of Dental Medicine, Columbia University Medical Center, New York, NY 10032, USA
[4]Department of Otolaryngology, Union Hospital, Tongji Medical College, Huazhong University of Science and Technology, Wuhan 430022, China
[5]Co-first author
*Correspondence: lily-c1030@163.com
https://doi.org/10.1016/j.stemcr.2017.11.017

SUMMARY

Skeletal mandibular hypoplasia (SMH), one of the common types of craniofacial deformities, seriously affects appearance, chewing, pronunciation, and breathing. Moreover, SMH is prone to inducing obstructive sleep apnea syndrome. We found that brain and muscle ARNT-like 1 (BMAL1), the core component of the molecular circadian oscillator, was significantly decreased in mandibles of juvenile SMH patients. Accordingly, SMH was observed in circadian-rhythm-disrupted or BMAL1-deficient mice. RNA sequencing and protein chip analyses suggested that matrix metallopeptidase 3 (MMP3) is the potential target of BMAL1. Interestingly, in juvenile SMH patients, we observed that MMP3 was obviously increased. Consistently, MMP3 was upregulated during the whole growth period of 3–10 weeks in *Bmal1*$^{-/-}$ mice. Given these findings, we set out to characterize the underlying mechanism and found BMAL1 deficiency enhanced *Mmp3* transcription through activating p65 phosphorylation. Together, our results provide insight into the mechanism by which BMAL1 is implicated in the pathogenesis of SMH.

INTRODUCTION

Skeletal mandibular hypoplasia (SMH), presenting with small mandibular deformity, results in an unfavorable facial profile (Hamid and Asad, 2003). In addition to affecting appearance, chewing, and pronunciation (de Almeida Prado et al., 2015; Maeda et al., 2008), severe SMH can cause narrowing of the pharyngeal airways, which results in obstructive sleep apnea syndrome (OSAS). OSAS increases the risks of cardiovascular disease, cerebrovascular events, depression, diabetes, and cognitive impairment, leading to poor life quality (Bibbins-Domingo et al., 2017; Gottlieb et al., 2010; Kendzerska et al., 2014; Peppard et al., 2006; Yaggi et al., 2005). Extensive studies on the pathogenesis of SMH have been conducted. Both hereditary and environmental factors contribute to SMH and its associated deformities (Bejdova et al., 2013; Boell and Tautz, 2011).

The circadian rhythm is of considerable interest because of its potential effects on tissue growth and development (Kaneshi et al., 2016). Circadian rhythm is an endogenous rhythm that allows organisms to adapt to the light-dark cycle, temperature changes, and other environmental factors, and it plays critical roles in many physiological and behavioral processes in mammals (Bailey et al., 2014; Bell-Pedersen et al., 2005). Previous studies have indicated that the metabolism of bone and cartilage shows a circadian manner, especially in the maxillomandibular complex (Dudek and Meng, 2014; Gafni et al., 2009). Moreover, circadian rhythms were seen in expression profiles of the master regulator gene of chondrogenesis, bone mineral deposition, and bone formation (Gafni et al., 2009; Maronde et al., 2010; McElderry et al., 2013; Takarada et al., 2012). Brain and muscle ARNT-like 1 (BMAL1) is the paramount component of the circadian rhythm molecular oscillator, and its functions are irreplaceable in maintaining the circadian oscillatory mechanism in mammals (Marcheva et al., 2010). Accumulating evidence suggests that BMAL1 plays pivotal roles in embryonic development and postnatal development, including oocyte fertilization, follicle development, angiogenesis, amelogenesis, neurodevelopment, hair growth, and intestinal regeneration (Al-Nuaimi et al., 2014; Jensen et al., 2012; Powell and LaSalle, 2015; Stokes et al., 2017; Xu et al., 2016b; Zhang et al., 2016; Zheng et al., 2013). The absence of BMAL1 can lead to multi-organ dysplasia, premature aging, and a shortened lifespan in mice (Xu et al., 2016b; Yang et al., 2016). In the skeletal system, BMAL1 can regulate bone and cartilage homeostasis and maintain structural integrity, and BMAL1 abnormal expression reduces bone mass significantly and predisposes knee cartilage to osteoarthritis-like damage (Dudek et al., 2016; Peek et al., 2017). It has been proven that BMAL1 deficiency in mice could result in limb bone hypoplasia (Samsa et al., 2016). However, there have been few studies on the effect of circadian rhythm or core clock gene *Bmal1* on mandibular development.

In this study, we found that BMAL1 expression in the mandibular tissues of juvenile patients with SMH decreased significantly compared with those of subjects with normal mandibular development. Furthermore, we noticed that the reduced mandibular bone formation was concomitant with decreased BMAL1 expression in circadian-rhythm-disrupted mice. Consistently, mandibular hypoplasia was observed in *Bmal1*$^{-/-}$ mice. To better understand the correlation between BMAL1 and mandibular hypoplasia, we deployed RNA sequencing and protein chip analyses and found that MMP3 was the potential target of BMAL1. In addition to promoting bone resorption (Flores-Pliego et al., 2015; Sundaram et al., 2007), MMP3 was verified to inhibit osteoblast differentiation of mouse bone mesenchymal stem cells (mBMSCs) to ensure the proper bone formation process. Surprisingly, chromatin immunoprecipitation (ChIP) and luciferase reporter assays showed that BMAL1 could not associate directly with the *Mmp3* promoter. Normally, phosphorylated p65 can translocate into the nucleus and subsequently promote *Mmp3* transcription (Souslova et al., 2010). Notably, we found that p65 was concentrated in the nucleus of BMAL1-depleted cells, suggesting that BMAL1 could impede the nuclear translocation of p65 via inhibiting p65 phosphorylation. Indeed, circadian locomotor output cycles kaput (CLOCK) can phosphorylate p65 in the absence of BMAL1, and BMAL1 addition can counteract the CLOCK-dependent activation of p65 (Spengler et al., 2012). Taken together, our results indicated that BMAL1 controls the expression of MMP3 indirectly via p65 phosphorylation modulation. Also, these results provided insight into the pathogenesis of SMH, presenting a potential therapeutic strategy of mandibular deformity.

RESULTS

BMAL1 Expression Is Downregulated in the Mandibular Tissues of Juvenile SMH Patients

SMH patients are characterized by the insufficient bone mass in the mandibles (Figure 1A). Reconstructed three-dimensional (3D) cone-beam computed tomography (CT) images showed the differences in bone mass between juvenile SMH patients and normal subjects (Figure 1B). In juvenile SMH patients, the indexes of mandibular growth Co-Go (right), Co-Go (left), Go-Me (right), and Go-Me (left) were significantly lower than those of the control group. Consistently, the indexes of the mandibular plane angle (MP)-Frankfurt horizontal (FH; right), MP-FH (left), were larger (Figure 1C).

To determine the correlation between the expression of clock genes and SMH, we used qRT-PCR and western blot to measure BMAL1, CLOCK, REV-ERBα, PER1, PER2, CRY1, and CRY2 expression levels in human mandibular tissues. The mRNA and protein levels of BMAL1, CLOCK, PER1, and CRY2 decreased significantly in the mandibular tissues of SMH patients, but the CRY1 expression was obviously upregulated (Figures 1D and 1E). These results suggested that circadian rhythm disruption could be involved in the pathogenesis of SMH. Notably, BMAL1 expression change is relatively prominent among the clock genes affected. The core clock gene *Bmal1* is an essential part of the circadian clock and has been implicated in maintaining circadian rhythm (Lipton et al., 2015). Indeed, BMAL1 has been reported to be involved in the development of limb bone (Samsa et al., 2016).

Circadian Rhythm Disruption Results in Decreased Mandibular Bone Mass and Bone Size

Our findings indicated that SMH is closely correlated with the expression changes of clock genes, suggesting that circadian rhythm may be involved in regulating bone development. To further determine if circadian rhythm participates in mandibular bone development specifically, we established a jet-lag mouse model to observe the impact of circadian rhythm disruption on the occurrence and development of SMH. In our experiment, C57BL/6J mice were placed under a normal 12 hr light/12 hr dark (LD12:12) or a jet-lag schedule with light advanced 8 hr every 2–3 days for 4 or 8 weeks (Figure 2A). By measuring the expression of clock genes at different time points, we verified that the jet-lag schedule disrupted the mouse circadian rhythm (Figure 2B). The mandibles of jet-lagged mice appeared grossly smaller than those of control mice (Figures 2C and 2D). Micro-CT analysis showed that the bone volume/total volume (BV/TV) and trabecular thickness (Tb.Th) were significantly decreased in the condylar regions of the jet-lagged group. 3D reconstructions demonstrated that the total length of the mandible and the height of the coronoid process were reduced in the jet-lagged group (Figure 2E). Also, additional indexes were also affected, such as BS/BV and bone mineral density (BMD), in the jet-lagged group (Figure S2). Serial sections of the mandibular tissues stained with Masson's trichrome and H&E showed that both the bone mass and the number of osteocytes in the jet-lagged group were decreased. Moreover, tartrate-resistant acid phosphatase (TRAP) staining displayed the increased number of osteoclasts compared with the LD12:12 group (Figures 2F and 2G). Together, these results suggest that circadian rhythm disruption is closely correlated with the decreased mandibular bone mass.

Loss of BMAL1 Leads to Skeletal Mandibular Hypoplasia

Thus far, our data suggest that circadian rhythm is implicated in mandibular bone development. Notably, BMAL1

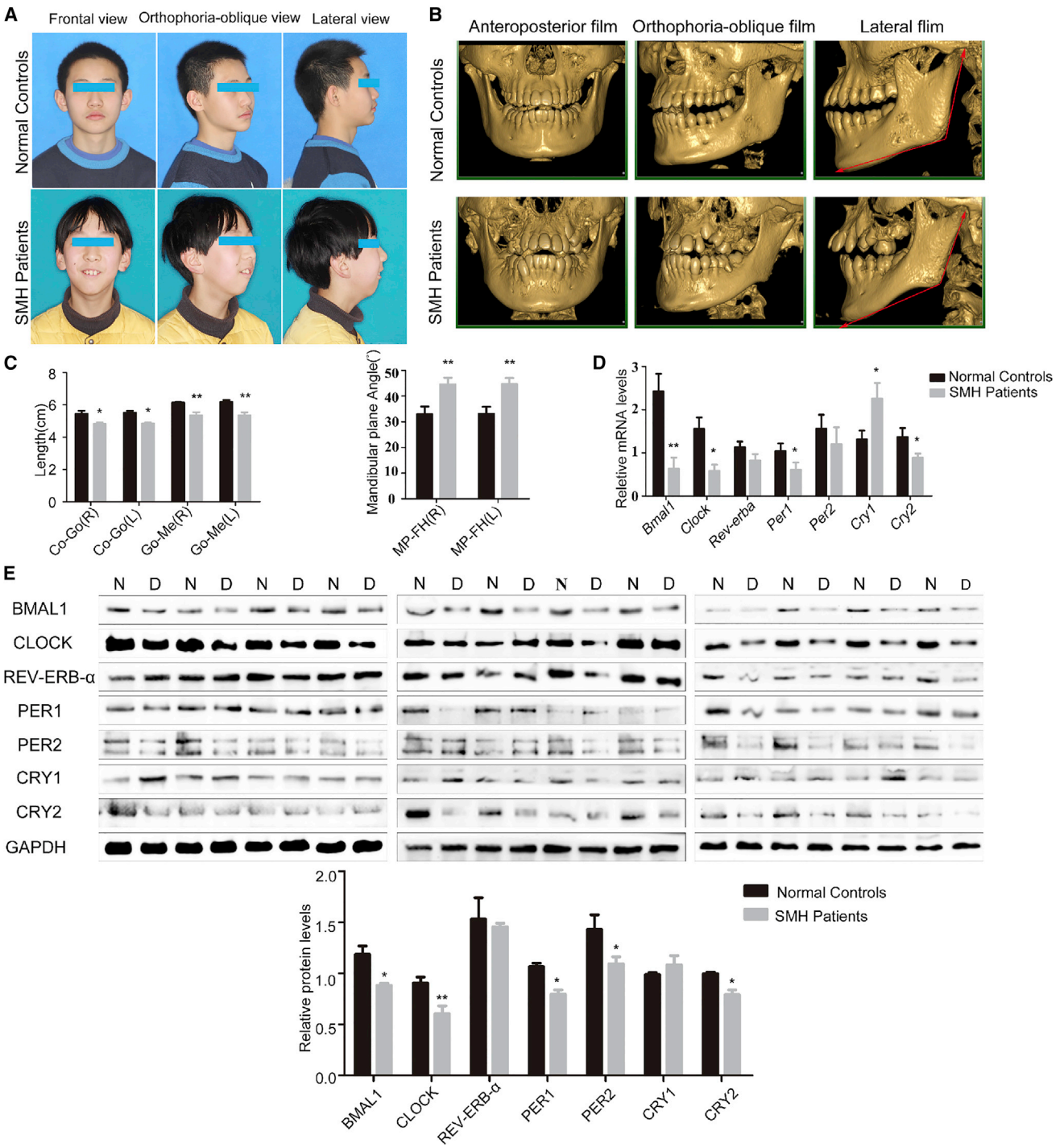

Figure 1. BMAL1 Expression Is Downregulated in the Mandibles of Juvenile SMH Patients

(A) The initial facial photographs of normal and SMH patients.

(B) Three-dimensional cone-beam computed tomography images of normal and SMH patients. In the lateral film, the red arrows refer to Co-Go (ramus length, distance between Co and Go) and Go-Me (distance between point Go and point Me).

(C) Comparisons of the bilateral lengths of Co-Go, Go-Me, and mandibular plane angle between SMH patients and normal individuals.

(D) qRT-PCR analysis of Bmal1, Clock, Rev-erbα, Per1, Per2, Cry1, and Cry2.

(E) Western blot analysis of BMAL1, CLOCK, REV-ERBα, PER1, PER2, CRY1, and CRY2 proteins.

Data represent the mean ± SD (n = 12 individuals per group). *$p < 0.05$ and **$p < 0.01$ (compared with control), from Student's t tests.

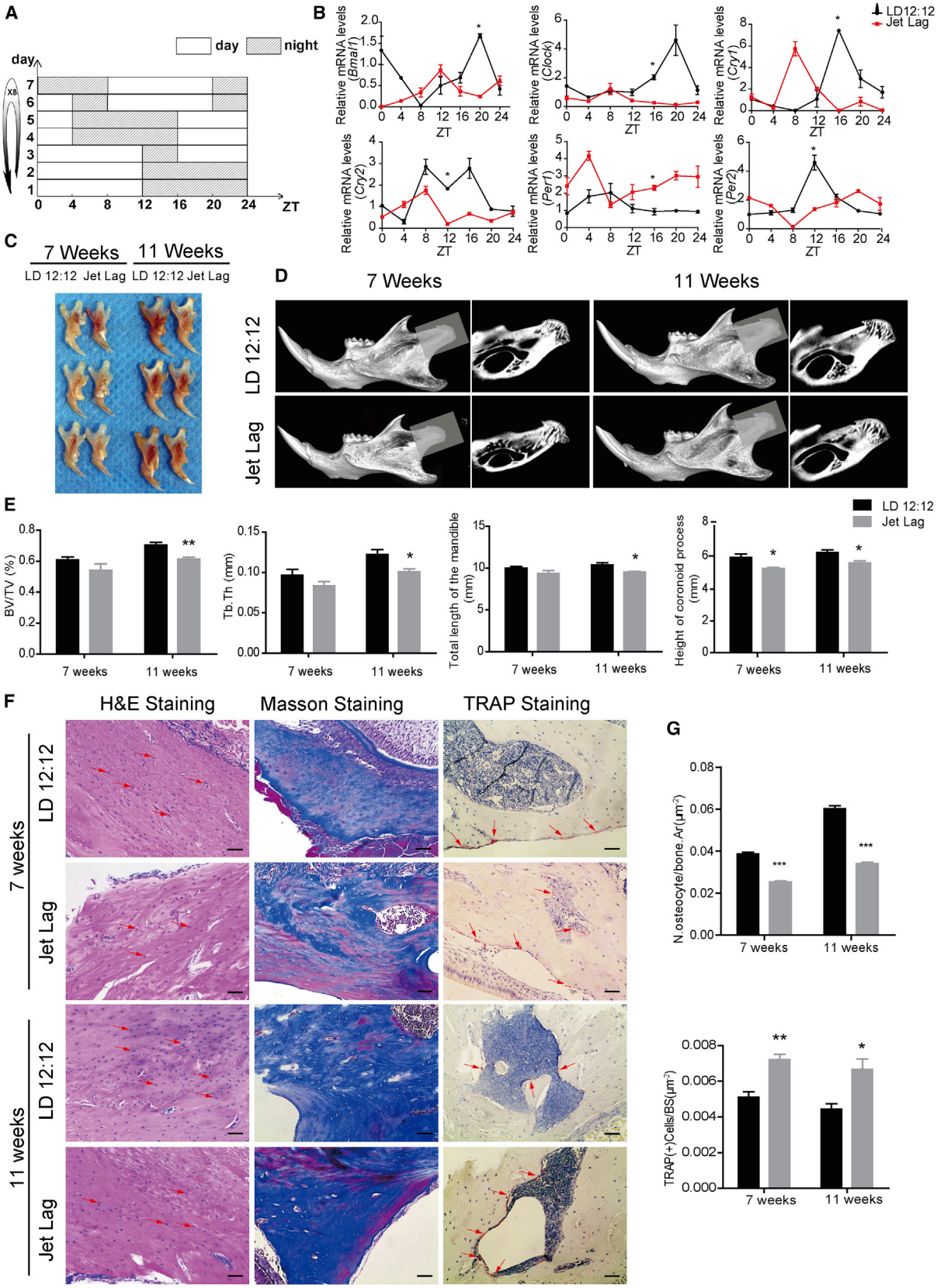

(legend on next page)

expression was affected prominently in SMH patients. To establish the role of BMAL1 in SMH, we constructed *Bmal1*$^{-/-}$ mice and confirmed their genotype by PCR (Figure 3A). The mandibles of *Bmal1*$^{-/-}$ mice are smaller than those of even-aged wild-type mice in 3- and 7-week-old animals (Figure 3B). Micro-CT analysis showed that BV/TV and Tb.Th of the condylar region of the mandible of *Bmal1*$^{-/-}$ mice were significantly reduced compared with those of the even-aged wild-type mice. Also, the total height of the mandible and height of the coronoid process were decreased upon loss of BMAL1 (Figures 3C and 3D). Moreover, additional indexes were also affected, such as BS/BV and BMD, in the *Bmal1*$^{-/-}$ mice (Figure S3). The results of Masson's staining showed that the mandibular bone mass of *Bmal1*$^{-/-}$ mice decreased significantly (Figures 3E and 3F). Similarly, the number of osteocytes per unit area declined in *Bmal1*$^{-/-}$ mice (Figures 3E and 3F). Moreover, the number of osteoclasts increased in *Bmal1*$^{-/-}$ mice (Figures 3E and 3F). The results of micro-CT analysis and H&E staining in the femur also showed decreased bone mass and osteocytes in *Bmal1*$^{-/-}$ mice (Figure S4), which are consistent with the results in mandibles. Taken together, these data indicated that BMAL1 deficiency led to bone dysplasia, probably by destroying the balance between bone formation and bone resorption.

BMAL1 Deficiency Inhibits Osteoblast Differentiation and Promotes Osteoclast Differentiation *In Vitro*

To test whether BMAL1 has intrinsic functionality in the osteogenic functions of mBMSCs, we extracted primary bone mesenchymal stem cells from *Bmal1*$^{-/-}$ and wild-type mice and performed Alizarin red S (ARS) staining. We noticed that the mineralization of mBMSCs from *Bmal1*$^{-/-}$ mice was significantly decreased (Figure 3G). We also tested the influence of BMAL1 on the osteoclast differentiation of RAW264.7 cells and found that short hairpin RNA (shRNA)-mediated knockdown of *Bmal1* effectively promoted osteoclast differentiation of the cells (Figure 3H). Taken together, these data indicated that BMAL1 deficiency restrained osteoblast differentiation and enhanced osteoclast differentiation simultaneously. In addition, our results verified that osteoclasts, osteocytes, and their precursor cells are specifically modulated by BMAL1 during SMH formation.

MMP3 Expression Is Prominently Upregulated in Mandibular Tissues of *Bmal1*$^{-/-}$ Mice

To gain an independent assessment of the regulatory targets of BMAL1, we performed genome-wide RNA sequencing (RNA-seq) to acquire the transcriptional profile in *Bmal1*$^{-/-}$ mBMSCs (Figure 4A). A total of 537 genes were found to be differentially expressed in BMAL1-depleted mBMSCs, including 227 downregulated genes and 310 upregulated genes (Figure 4B). Importantly, many candidate genes are osteogenesis-related and/or osteoclastic-related genes (Figure 4C). We further performed qRT-PCR to validate these differentially expressed osteogenesis-related or osteoclast-related genes in *Bmal1*$^{-/-}$ mBMSCs (Figure 4D). Furthermore, we performed protein chip assays of mandible tissues from 3-, 4-, 5-, 6-, 7-, 8-, 9-, and 10-week-old mice. The results showed that MMP3 expression upregulation is prominent and consistent throughout the growth period in the mandibular tissues of *Bmal1*$^{-/-}$ mice (Figure 4E and Table S3). Western blot confirmed the same trend of MMP3 level change (Figure 4F). Together these results suggested that MMP3 is a potential regulatory target of BMAL1 during SMH.

MMP3 Is Negatively Correlated with BMAL1 during Osteoblast Differentiation and Osteoclast Differentiation

To better understand the mechanisms by which BMAL1 and its potential target MMP3 modulate mandibular growth, we analyzed the expression level of MMP3 from mandibular tissues of juvenile SMH patients and normal peers. We observed that MMP3 expression level was

Figure 2. Circadian Rhythm Disruption Results in Decreased Mandibular Bone Mass and Bone Size

(A) The schematic shows the timeline of the jet-lag experiment schedule used to establish the mouse model of circadian rhythm disruption.

(B) qRT-PCR analysis demonstrated successful establishment of the mouse model (n = 5 animals per time point).

(C) Photograph of the mandibles of 7- and 11-week-old male C57BL/6J mice under normal LD12:12 or jet-lag conditions.

(D) Representative images of micro-CT reconstruction of mandibles in normal and jet-lagged circadian-rhythm-disrupted mice. The shadows indicate the position of the condylar regions.

(E) Micro-CT analysis of bone volume/total volume (BV/TV), trabecular thickness (Tb.Th), the total length of the mandible, and the height of coronoid process (n = 5 per group).

(F) Representative images of H&E, Masson's trichrome, and TRAP staining in the mandibles of normal and jet-lagged circadian rhythm-disrupted mice. The arrows in the H&E staining images indicate osteocytes, and arrows in the TRAP staining images indicate osteoclasts. Scale bar, 50 μm.

(G) Osteocyte number (N.Osteocyte/Bone.Ar) and osteoclast number (TRAP(+) cells/BS) in mandible sections (n = 5 per group).

Data represent the mean ± SD. *p < 0.05, **p < 0.01, and ***p < 0.001 (compared with control), from Student's t tests.

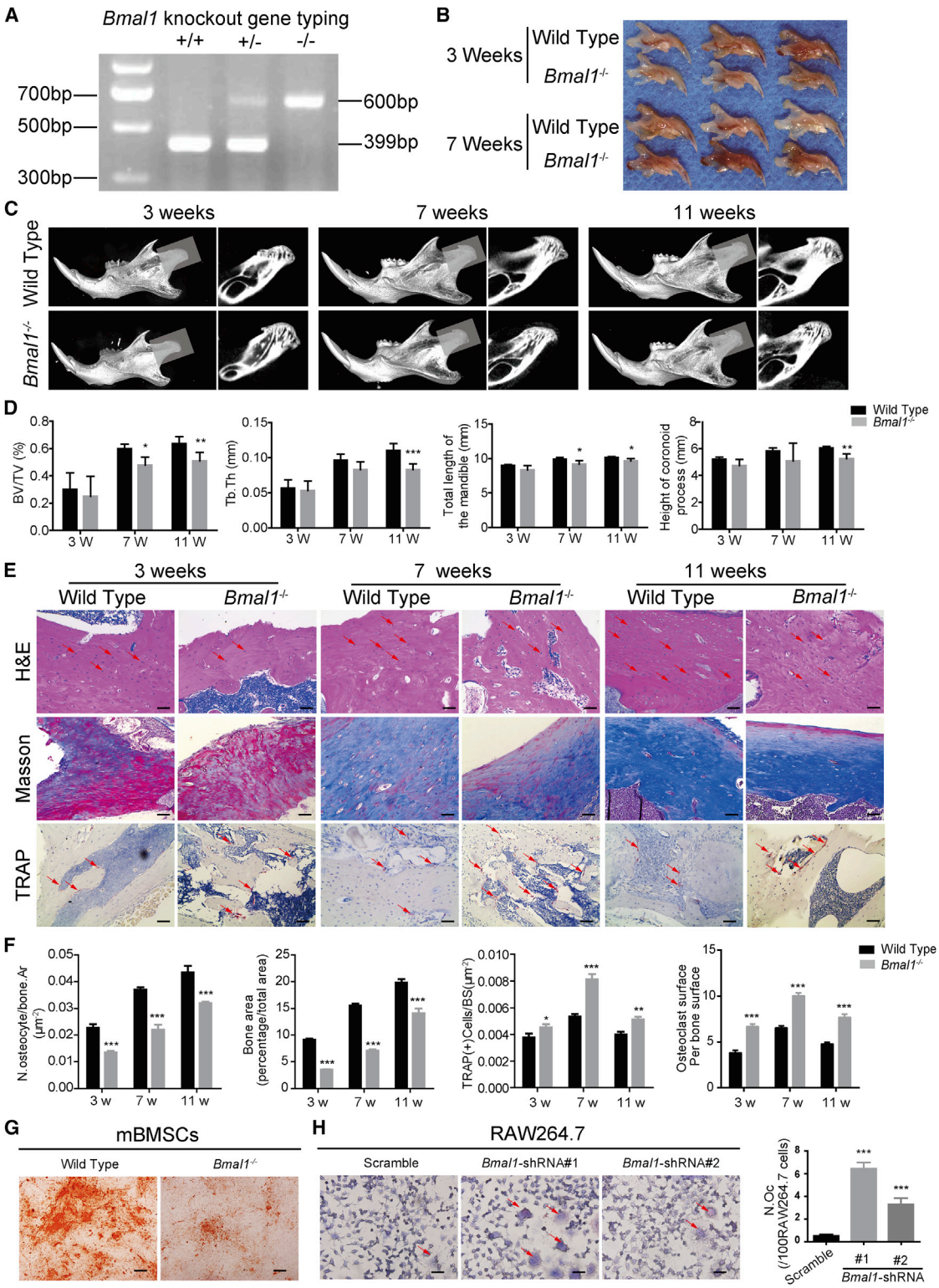

Figure 3. Loss of BMAL1 Leads to Skeletal Mandibular Hypoplasia

(A) The genotypes of *Bmal1*$^{-/-}$, *Bmal1*$^{+/-}$, and *Bmal1*$^{+/+}$ mice determined by PCR (n = 5 per genotype).

(B) Photograph of the mandibles of 3- and 7-week-old male wild-type and *Bmal1*$^{-/-}$ mice.

(legend continued on next page)

significantly upregulated and presented a negative correlation with BMAL1 level change in the SMH patients (Figure 5A). Protein chip analysis showed the elevated expression of MMP3 was consistent throughout the entire growth period in *Bmal1*$^{-/-}$ mice (Figures 4E and 4F). Consistently, the MMP3 protein level in 3-, 7-, and 11-week-old *Bmal1*$^{-/-}$ mandibular tissue was higher than that in wild-type mice (Figure 5B). Also, the level of MMP3 was greatly upregulated in BMAL1 knockout mBMSCs, BMAL1 knockdown MC3T3-E1 cells, and RAW264.7 cells. Conversely, MMP3 was downregulated in BMAL1-overexpressing MC3T3-E1 cells (Figures 5C, 5D, and S5A–S5C). These results suggested that MMP3 could be an important regulatory target of BMAL1.

We then used mBMSCs and RAW264.7 cells to assay the effect of MMP3 level variation on osteoblast differentiation and osteoclast differentiation, respectively. Indeed, there was an evident increase of osteoblast differentiation in mBMSCs upon depletion of MMP3 by transfection with lentivirus vectors encoding shRNA targeting *Mmp3* (Figures 5E and 5F). Similarly, increased osteoblast differentiation was observed in the MMP3-specific inhibitor $C_{27}H_{46}N_{10}O_9S$-treated mBMSCs (Figure 5G). Next, we found that MMP3 knockdown RAW264.7 cells exhibited impaired osteoclast differentiation, as indicated by TRAP staining. Decreased osteoclast differentiation was also observed in RAW264.7 cells treated with the MMP3-specific inhibitor (Figures 5H–5J). Importantly, BMAL1 knockdown-induced osteoclast differentiation enhancement was significantly reversed by shRNA-mediated MMP3 knockdown (Figure 5K). Taken together, these results indicated that MMP3 upregulation is involved in mandibular hypoplasia caused by BMAL1 deficiency.

Suppression of BMAL1-Mediated MMP3 Expression Requires p-p65

The well-known transcription factor BMAL1 performs its functions by activating the transcription of downstream target genes, including matrix metalloproteinases (MMPs) (Huang et al., 2012; Lou et al., 2017). To test whether upregulated MMP3 expression and secretion are due to the direct transcription activation of *Mmp3*, a ChIP assay was performed in MC3T3-E1 cells. Surprisingly, we found that BMAL1 does not regulate MMP3 expression directly (data not shown). Recent studies revealed that the phosphorylation of p65 (a subunit of nuclear factor κB [NF-kB]) and its nucleus translocation are required for the transcriptional regulation of NF-κB downstream genes, including *Mmp3* (Souslova et al., 2010; Spengler et al., 2012). Interestingly, we found that the phosphorylation level of p65 was significantly affected in BMAL1-overexpressing or BMAL1 knockdown mBMSCs (Figure 6A). To determine whether p65 is involved in the mandibular hypoplasia, we assayed the p65 knockdown effects on osteoblast differentiation of mBMSCs and osteoclast differentiation of RAW264.7 cells. We observed that shRNA-mediated p65 knockdown increased osteoblast differentiation of mBMSCs and decreased osteoclast differentiation of RAW264.7 cells (Figures 6B and 6C). We speculated that p65 could be an essential functional link between BMAL1 and MMP3. Indeed, P-p65 protein transportation to the nucleus was increased in both BMAL1 knockdown RAW264.7 cells and BMAL1 knockdown MC3T3-E1 cells (Figures 6D and S6). It was reported that P-p65 protein relocation to the nucleus could activate the transcription of downstream genes (Perkins, 2006). Consistently, p65 knockdown inhibited MMP3 expression in MC3T3-E1 cells (Figure 6E). In addition, the ChIP and luciferase reporter assays demonstrated that p65 binds to the *Mmp3* promoter and activates *Mmp3* transcription in MC3T3-E1 cells (Figures 6F and 6G). In Figure 6G, we showed that knockdown of p65 inhibited the activity of the *Mmp3* promoter but not those of mutants with the p65 binding site being deleted or mutated. Together these findings suggested that BMAL1 deficiency contributes to mandibular dysplasia via upregulating MMP3 expression, and BMAL1-mediated MMP3 expression inhibition requires p65 phosphorylation and transportation to the nucleus.

(C) Representative images of micro-CT reconstruction of the mandibles in 3-, 7-, and 11-week-old wild-type and *Bmal1*$^{-/-}$ mice. The shadows indicate the positions of the condylar regions.
(D) Micro-CT analysis of bone volume/total volume (BV/TV), trabecular thickness (Tb.Th), the total length of the mandible, and the height of coronoid process (n = 5 per group).
(E) Representative images of H&E, Masson's trichrome, and TRAP staining of the mandibles of 3-, 7-, and 11-week-old wild-type and *Bmal1*$^{-/-}$ mice. Arrows in the H&E staining imagings indicate osteocytes, and arrows in the TRAP staining images indicate osteoclasts. Scale bar, 50 μm.
(F) Osteocyte number (N.Osteocyte/Bone.Ar), bone area, osteoclast number (TRAP(+) cells/BS), and osteoclast surface per bone surface in mandible sections (n = 5 per group).
(G) Representative images of ARS staining of mBMSCs (n = 3 independent experiments). Scale bar, 100 μm.
(H) Representative images of TRAP staining in RAW264.7 cells. Scale bar, 25 μm. Arrows in the TRAP staining images indicate osteoclasts, and the number of osteoclasts was counted (n = 3 independent experiments).
Data represent the mean ± SD. *p < 0.05, **p < 0.01, and ***p < 0.001 (compared with control), from Student's t tests.

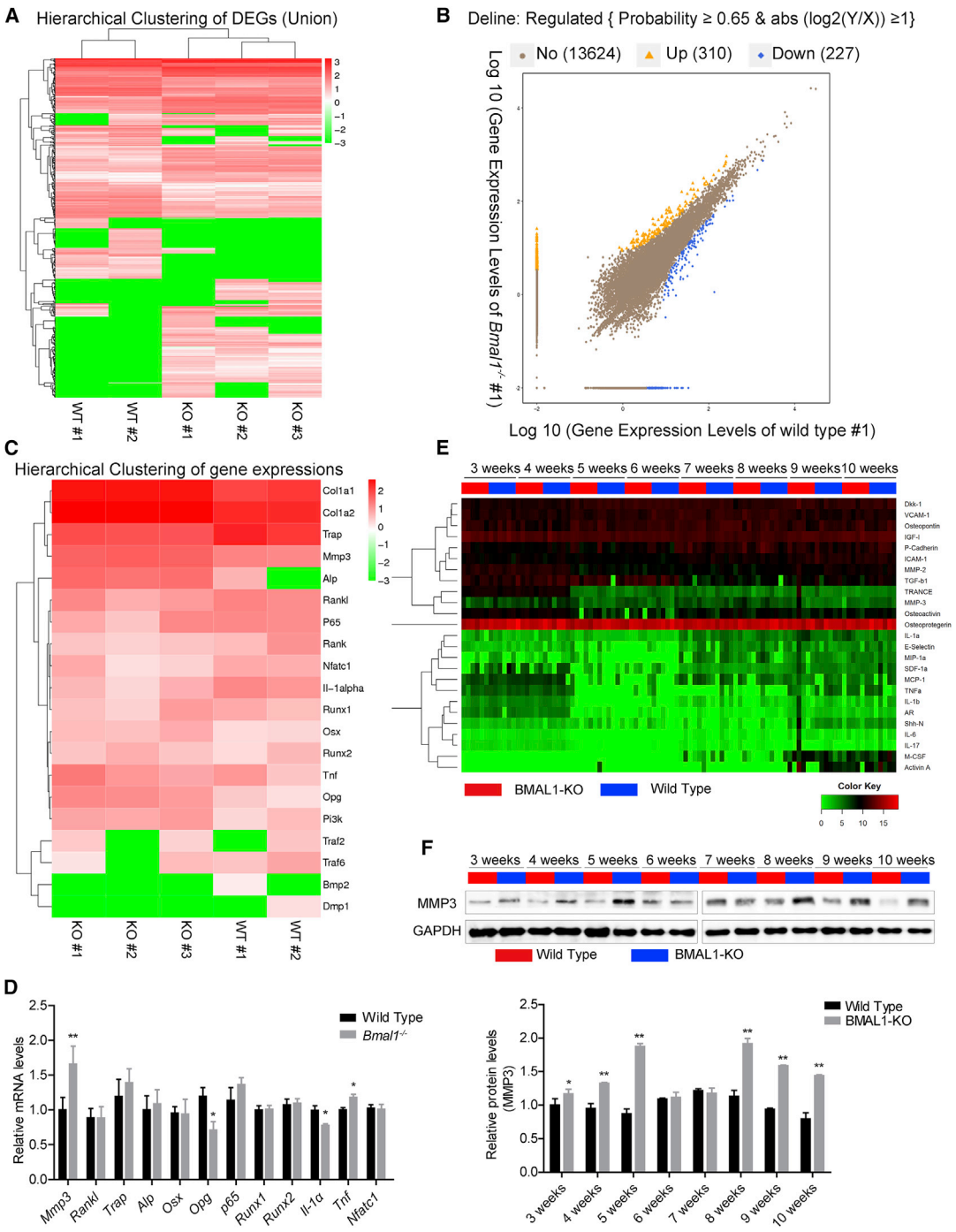

Figure 4. MMP3 Expression Is Prominently Upregulated in Mandibular Tissues of *Bmal1*$^{-/-}$ Mice

(A) Hierarchical clustering of quantitative gene expression profiling for mandibular tissues in wild-type and *Bmal1*$^{-/-}$ mice.

(B) Volcano plot of differentially expressed genes (DEGs) in mandibular tissues between wild-type and *Bmal1*$^{-/-}$ mice.

(C) Heatmap shows DEGs related to bone development.

(D) Confirmation of the DEGs by qRT-PCR (n = 5 independent experiments). All genes tested followed the expression pattern identified by RNA-seq.

(E) Heatmap shows the results of protein microarray (n = 6 pairs per week).

(F) Western blot verified the expression changes of MMP3 proteins (n = 6 per group).

Data represent the mean ± SD. *p < 0.05 and **p < 0.01 (compared with control), from Student's t tests.

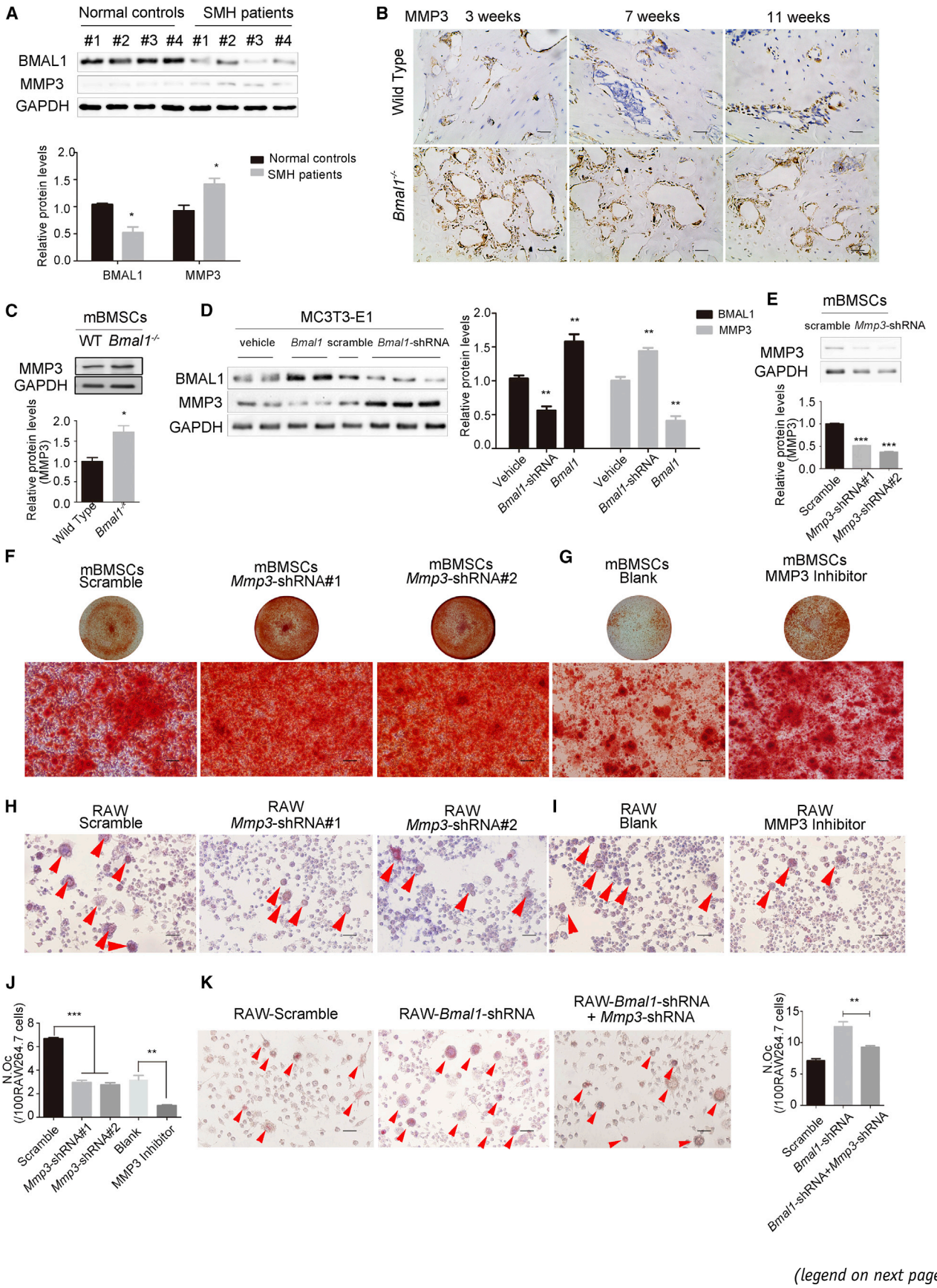

(legend on next page)

DISCUSSION

Circadian rhythm, the inherent rhythm of the body, evolved to adapt to long-term changes in light, temperature, and other environmental factors (Dibner and Schibler, 2015; Gerhart-Hines and Lazar, 2015). Circadian rhythm plays essential roles in various physiological and pathological processes, including bone growth and bone resorption (Bass and Takahashi, 2010; Fu et al., 2005; Panda et al., 2002; Xu et al., 2016a). In this study, we found that juvenile SMH patients have abnormal circadian clock gene expression in the mandibular tissues. In jet-lagged mice, we observed reduced mandible bone mass and bone size, suggesting that circadian rhythm deficiency is a risk factor for the occurrence of mandibular hypoplasia. Circadian rhythm was greatly affected by changes in habitation and living habits (Kohyama, 2014; Wyse et al., 2014). Noise, light, personal habits, depression, and sleep disorders often affect circadian rhythm severely (Basner et al., 2014; Bedrosian and Nelson, 2013; Landgraf et al., 2015; Munzel et al., 2014; Parry et al., 2008). Circadian rhythm dysfunction has been suggested to be associated with various human diseases, such as cardiovascular disease, diabetes, cancer, and developmental malformations (Muller and Tofler, 1991; Potocki et al., 2000; Tamemoto, 2012; Tang et al., 2017). BMAL1 is a core component that plays critical roles in generating and maintaining circadian rhythm (Lipton et al., 2015). BMAL1 deficiency had a broad impact on bone deformity, which is consistent with the previous reports (Min et al., 2016; Samsa et al., 2016). Consistently, we observed that juvenile SMH patients had decreased BMAL1 expression in their mandibular tissues. In *Bmal1*$^{-/-}$ mice, mandible bone mass and bone size were also reduced. The mandible arises from neural crest stem cells of the neuroectoderm germ layer rather than the mesoderm (Chai and Maxson, 2006). The mandible is remodeled faster than the other bones (Huja et al., 2006). Interestingly, our study demonstrated essential roles of BMAL1 and circadian rhythm during the growth and development of the mandible.

MMPs were identified as collagen-cleaving soluble proteases (Aiken and Khokha, 2010). MMP1, MMP9, and MMP13 are required for development and maintenance of osteocyte processes. Especially, MMP3 was found to be implicated in bone remodeling and degrading cartilage (Eguchi et al., 2008; Garcia et al., 2013; Holmbeck et al., 2004; Li et al., 2015a). We found that MMP3 was upregulated in mandibular tissues of juvenile SMH patients. The previous study reported that BMAL1 promotes osteoblast differentiation by upregulating BMP2 expression, indicating the correlation of BMAL1 with osteoblast differentiation regulators (Min et al., 2016). Together these results highlight the complex mechanism of circadian-rhythm-related bone developmental processes.

Being a transcription factor, BMAL1 regulates gene expression by activating the gene promoter. However, ChIP and luciferase reporter assays showed that BMAL1 does not bind directly to the *Mmp3* promoter (data not shown). Intriguingly, Spengler et al. (2012) reported that p65, a critical subunit for NF-κB transactivation, was required for the BMAL1-mediated suppression of downstream gene transcription. Also, *Bmal1* targeting by miR-155 could lead to a pro-inflammatory state by activating p65 (Curtis et al., 2015). Hence, we sought to determine the correlation among BMAL1, p65, and MMP3. We found that the phosphorylated level of p65 is tightly associated with MMP3 expression in BMAL1-overexpressing or BMAL1 knockdown MC3T3-E1 cells. It is

Figure 5. MMP3 Is Negatively Correlated with BMAL1 during Osteoblast Differentiation and Osteoclast Differentiation

(A) Western blot analysis of MMP3 protein expression in human mandibles with SMH compared with normal individuals (n = 12 individuals per group).

(B) Immuno-histochemical staining verified increased expression of MMP3 in mandibular tissues of *Bmal1*$^{-/-}$ mice (n = 5 per group). Scale bar, 25 μm.

(C) Western blot analysis of MMP3 in *Bmal1*$^{-/-}$ mBMSCs (n = 3 independent experiments).

(D) Western blot analysis of BMAL1 and MMP3 in BMAL1-overexpressing or BMAL1 knockdown MC3T3-E1 cells (n = 3 independent experiments).

(E) The knockdown of MMP3 by shRNA was confirmed by western blotting (n = 3 independent experiments).

(F and G) Representative ARS staining images of MMP3 knockdown mBMSCs or mBMSCs treated with the MMP3 inhibitor $C_{27}H_{46}N_{10}O_9S$ (n = 3 independent experiments). Scale bar, 100 μm.

(H–J) Representative TRAP staining images of MMP3 knockdown RAW264.7 cells or cells treated with MMP3 inhibitor $C_{27}H_{46}N_{10}O_9S$. Scale bar, 50 μm. Arrowheads in the TRAP staining images indicate osteoclasts, and the number of osteoclasts was counted (n = 3 independent experiments).

(K) Representative TRAP staining images of RAW264.7 cells, BMAL1 knockdown RAW264.7 cells, and BMAL1 and MMP3 double-knockdown RAW264.7 cells. Scale bar, 50 μm. Arrowheads in the TRAP staining images indicate osteoclasts, and the number of osteoclasts was counted (n = 3 independent experiments).

Data represent the mean ± SD, *$p < 0.05$, **$p < 0.01$, and ***$p < 0.001$. Two-tailed Student's t test (A, C–E, and J) and ANOVA with Tukey's post hoc test (K) were used.

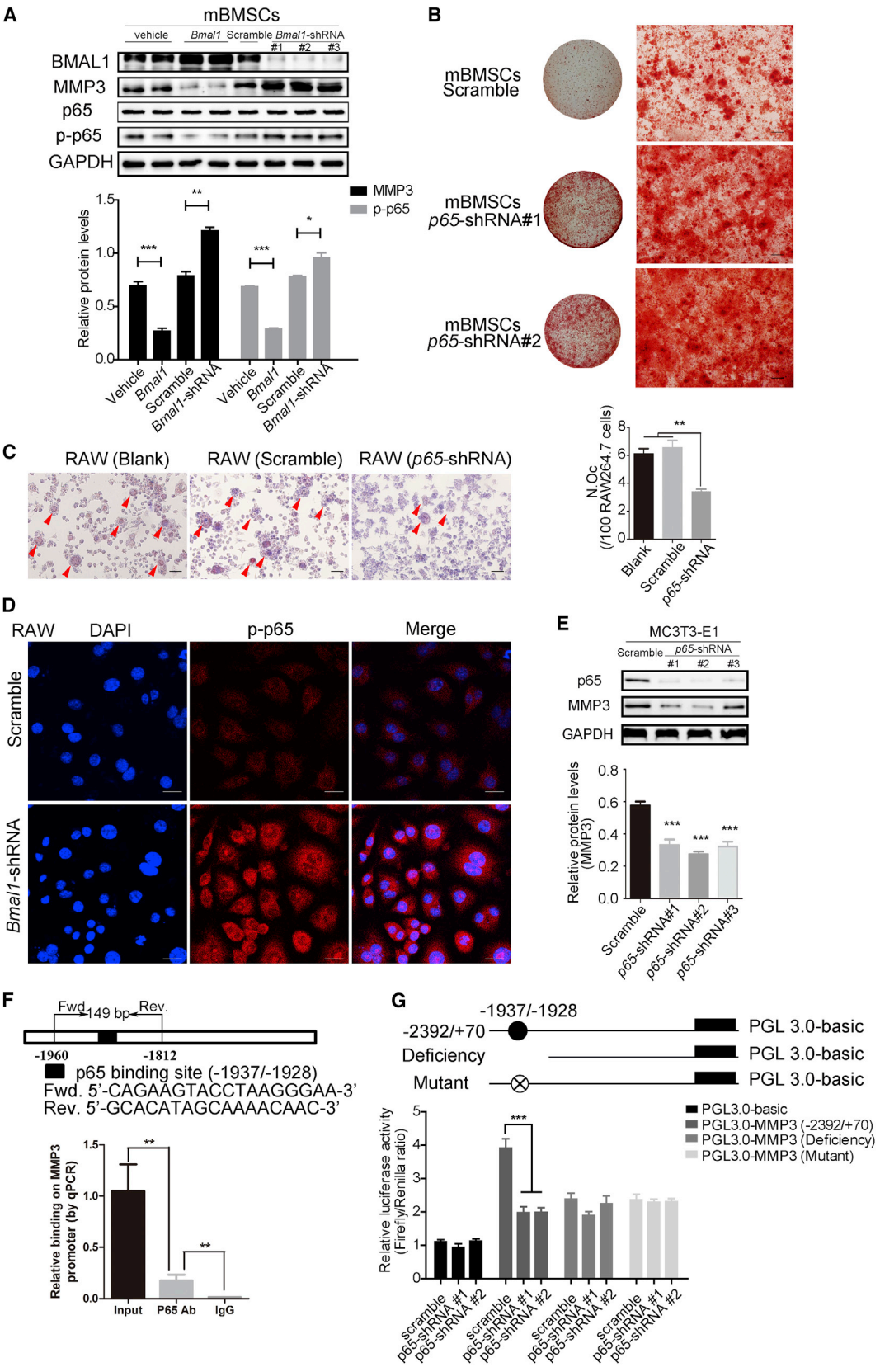

(legend on next page)

widely acknowledged that phosphorylated p65 translocates to the nucleus and activates transcription (Perkins, 2006). Indeed, we found that p-p65 could promote *Mmp3* transcription via direct binding to the promoter.

MMP3 is an endogenous activator of MMP9 (Flores-Pliego et al., 2015), which is the most abundant MMP member implicated in osteoclast differentiation and recruitment (Sundaram et al., 2007). MMP3 triggers the release of tumor necrosis factor alpha (TNF-α), which stimulates MMP9 production through activating the MAPK/ERK1/2 signaling pathway (Steenport et al., 2009; Van den Steen et al., 2002). MMP9 then activates RANKL-induced osteoclast differentiation (Franco et al., 2011). In mBMSCs, we found that MMP3 could inactivate the MAPK/ERK pathway and the phosphatidylinositol 3 kinase (PI3K)/AKT pathway (data not shown), which are in close positive correlation with osteoblast differentiation (Li et al., 2015b, 2017). Therefore, we speculate that BMAL1 regulates osteoblast differentiation by manipulating MMP3 and the downstream signaling pathways.

Collectively, our data demonstrates that MMP3 is an indispensable factor in BMAL1-deficiency-induced mandibular dysplasia and provides insight into the mechanism of mandibular deformities. Moreover, our results provided a valuable reference for juveniles to correct undesirable effects on lifestyle.

EXPERIMENTAL PROCEDURES

Patient Tissue Specimens

Twenty-four human mandibular specimens were obtained from patients at the Wuhan Union Hospital, Tongji Medical College, Huazhong University of Science and Technology (Wuhan, China) from May 2014 to June 2015. Tissue specimens were obtained between 9:00 am and 11:00 am at consistent time points. Twelve specimens were acquired from juvenile patients with SMH, and another 12 normal specimens were collected from sex-matched control peers. All subjects were between 10 and 12 years old, and their skeletal maturation preceded the advent of the growth and development peak determined by the quantitative cervical vertebral maturation method. Clinical characteristics, including age, sex, and body mass index, are shown in Table S1, and there were no significant differences. Subjects were selected for the experimental group according to the following inclusion criteria: convex facial type, class II disocclusion, skeletal mandibular dysplasia, lateral cephalometric radiograph showing a sella-nasion-A-point (SNA) angle of 82.3° ± 3.5°, sella-nasion-B-point (SNB) angle <73.8°, A-point-nasion-B-point (ANB) angle >5°. Subjects were selected to the control group according to the following inclusion criteria: normal facial shape, normal maxillary and mandibular development, lateral cephalometric radiograph showing an SNA angle of 82.3° ± 3.5°, SNB angle of 77.6° ± 2.9°, 1° < ANB angle <5°. Subjects with temporomandibular joint disorder, history of maxillofacial trauma, or orthodontic treatment were excluded.

Animals

A total of 140 male C57BL/6J mice were obtained from Beijing HFK Bioscience (Beijing, China) and fed antibiotic-free food and water *ad libitum*. Mice were placed randomly under either LD12:12 conditions with the light on from 8:00 a.m. (this timing set as zeitgeber time 0 [ZT0]) to 8:00 p.m. (ZT12) or under a jet-lagged condition. For the jet-lagged group, animals were placed under alternating light-cycle conditions with light advanced 8 hr every 2–3 days for 4 or 8 weeks. After 4 and 8 weeks, five mice per time point were killed to obtain mandibular tissues at the indicated time points (ZT0, ZT4, ZT8, ZT12, ZT16, ZT20, and ZT24). Homozygous BMAL1-deficiency (*Bmal1*$^{-/-}$) mice in the C57BL/6J background were produced by breeding heterozygous BMAL1-deficiency mating pairs (*Bmal1*$^{+/-}$), which were kindly provided by Dr. Y. Xu (Soochow University, Jiangsu, China), and the BMAL1 deficiency was confirmed by multiplex PCR as described by Bunger et al. (2000).

Cell Culture, Flow Cytometric Analysis, Osteogenic Induction, and Osteoclastogenesis

MC3T3-E1 cells (ATCC) and RAW264.7 cells (ATCC) were cultured in minimum essential medium α (α-MEM; Cyagen, Guangzhou,

Figure 6. BMAL1-Mediated MMP3 Expression Suppression Requires p-p65

(A) Western blot analysis of MMP3 and phosphorylated p65 proteins in BMAL1-overexpressing or BMAL1 knockdown mBMSCs (n = 3 independent experiments).

(B) Representative ARS staining images of p65 knockdown mBMSCs (n = 3 independent experiments). Scale bar, 100 μm.

(C) Representative TRAP staining images of p65 knockdown RAW264.7 cells. Arrowheads in the TRAP staining images indicate osteoclasts, and the number of osteoclasts was counted (n = 3 independent experiments). Scale bar, 50 μm.

(D) Confocal microscopic images of P-p65 in BMAL1 knockdown RAW264.7 cells and scrambled shRNA-transfected cells (n = 3 independent experiments). Scale bar, 25 μm.

(E) Western blot analysis of MMP3 in p65 knockdown MC3T3-E1 cells (n = 3 independent experiments).

(F) The transcription factor p65 bound to the *Mmp3* promoter in MC3T3-E1 cells. Chromatin immunoprecipitation assays were performed using anti-p65 with anti-Ig G as a negative control (n = 3 independent experiments).

(G) A luciferase reporter assay was performed to measure the activities of wild-type *Mmp3* promoter (−2,392/+70), and the mutant promoter with p65 binding site deleted or mutated in p65 knockdown MC3T3-E1 cells and scrambled shRNA-transfected cells. Filled black circle, p65-binding site. Filled crossed black circle, mutation of p65-binding site (n = 3 independent experiments).

Data represent the mean ± SD, *p < 0.05, **p < 0.01, and ***p < 0.001. Two-tailed Student's t test (A, C, and E) and ANOVA with Tukey's post hoc test (F and G) were used.

China) supplemented with 10% fetal bovine serum (FBS) (Gibco, USA) and 1% penicillin-streptomycin (HyClone). The cells were isolated from the femur marrow of 6- to 8-week-old mice and cultured in α-MEM supplemented with 12% FBS. All cells were maintained at 37°C in a 5% CO_2 humidified incubator. Direct immunofluorescence-based flow cytometric analysis was performed to identify mBMSCs (Figure S1). The expression levels of CD11b, CD44, Sca-1, CD29, and CD45 were determined by flow cytometric analysis using APC/Cy7-labeled anti-CD11b (#101225, BioLegend), phycoerythrin (PE)-labeled anti-CD44 (#103007, BioLegend), PE-labeled anti-Ly6A/E (Sca-1) (#108107, BioLegend), fluorescein isothiocyanate-labeled CD29 (#102205, BioLegend), and PerCP/Cy5.5-labeled anti-CD45 (#103131, BioLegend), respectively. The corresponding isotype-matched conjugated irrelevant monoclonal antibodies were used as negative controls. Primary mBMSCs were plated at 1×10^6 cells/well in six-well plates to induce osteoblast differentiation using medium supplemented with 50 μg/mL ascorbic acid, 10 nmol/L dexamethasone, and 10 mmol/L β-glycerophosphate (Sigma). Cells were cultured for 14 days in either control or differentiation medium followed by fixation with 4% formaldehyde and staining with 1% ARS (Cyagen, Guangzhou, China). RAW264.7 cells were plated at 5×10^4/well in 12-well plates in α-MEM supplemented with 10% FBS and 50 ng/mL RANKL (R&D Systems, USA) for 5 days to induce osteoclastogenesis, and then the cells were stained with TRAP.

Micro-CT

After the hind limbs and mandibles were harvested from the mice, soft tissues were removed, and the bone tissues were fixed in 4% paraformaldehyde. Scanning was performed at a resolution of 9 μm using the Skyscan 1076 micro-CT (Inveon Multimodality Scanner; Siemens, Erlangen, Germany). The images were used to reconstruct the tomography scans and quantified by Inveon Research Workplace software. Bone mass was evaluated according to BMD, BV/TV, Tb.Th, BS/BV, and trabecular pattern factor (Tb.PF). Ramus angle, the height of the coronoid process, the total length of the mandible, and base length of the mandible were measured to evaluate mandible development, while the marrow cavity in the 0.5–1 mm range under the cortical bone of the fossa intercondyloidea was used to evaluate femur development.

RNA Sequencing

Total RNA was extracted from in *Bmal1*$^{-/-}$ and wild-type mBMSCs using Trizol reagent according to the manufacturer's protocol. The samples were sent to the Labs Biotech (Changchun, China) for quantification, preparation of the RNA-seq library, and sequencing. The Ion Total RNA-Seq Kit v2 (Thermo Fisher) was used to prepare the sequencing libraries. Then the final template-positive Ion PI Ion Sphere particles were enriched and loaded onto the Ion PI chip. Later, raw reads above the filtering threshold (≥50 bp) were chosen for mapping. Gene expression was quantified using RPKM (reads per kilobase of transcript per million mapped reads) values and corrected by the upper quartile.

Protein Chip

The protein samples were collected from the mandibular tissues of 3-, 4-, 5-, 6-, 7-, 8-, 9-, and 10-week-old *Bmal1*$^{-/-}$ mice and wild-type mice and were then used to assess 25 proteins using Quantibody Mouse Cytokine Arrays 2 (Ray-Biotech, Norcross, GA). Samples were loaded onto the wells of chips by the standards provided. The chips were performed according to the manufacturer's instructions and data were read with microarray analysis software (GenePix, ScanArray Express, ArrayVision, MicroVigene).

Other Methods

Immunohistochemistry and immunofluorescence, ELISA, direct co-cultures, viral infection, qRT-PCR analysis, western blot analysis, quantitative real-time RT-PCR analysis, ChIP assay, and luciferase reporter assay were performed using a standard protocol. See Supplemental Experimental Procedures for more details.

Study Approval

All animal-related procedures were performed according to the ethical guidelines of, and were approved by, the Institutional Animal Care and Use Committee of Tongji Medical College (Institutional Animal Care and Use Committee number 539). Human mandibular specimens were obtained from patients at the Department of Stomatology, Wuhan Union Hospital, Tongji Medical College, Huazhong University of Science and Technology (Wuhan, China) from May 2014 to January 2015. This study protocol was approved by the Institutional Research Ethics Committee of Tongji Medical College (Wuhan, China) (approval number 2014S05001). The study was performed in accordance with the Declaration of Helsinki. Written informed consents were obtained before data collection.

Statistical Analysis

All data are displayed as means ± SD. SPSS 17.0 (SPSS, Chicago, IL) was used for the statistical analyses. Data were evaluated by the two-tailed Student's t test or by ANOVA with Tukey's post hoc test for multiple comparisons. A p value <0.05 was considered significant.

ACCESSION NUMBERS

The accession number for the RNA sequencing data reported in this paper is GEO: GSE106586.

SUPPLEMENTAL INFORMATION

Supplemental Information includes Supplemental Experimental Procedures, six figures, and three tables and can be found with this article online at https://doi.org/10.1016/j.stemcr.2017.11.017.

AUTHOR CONTRIBUTIONS

L.C. designed the experiments and supervised the study; L.C., J.Z., X.Z., Q.T., R.Y., S.Y., and Y.L. conducted the experiments; J.Z., X.Z., Q.T., R.Y., S.Y., and Y.L. acquired the data; L.C., J.Z., X.Z., Q.T., R.Y., S.Y., C.C., J.H., A.S., J.J.M., and X.C. analyzed the data; L.C., J.Z., X.Z., and Q.T. wrote the manuscript.

ACKNOWLEDGMENTS

This work was funded by the National Science Fund for Excellent Young Scholars (31725011, to L.C.), the National Science Fund

for Outstanding Young Scholars (31422022, to L.C.), the National Natural Science Fund (31370980, to L.C.; 81700946, to J.Z.), and the Clinical Research Physician Program of Tongji Medical College, HUST. The authors thank Prof. Ying Xu of Soochow University for the heterozygous BMAL1-deficient mating pairs (*Bmal1*$^{+/-}$).

Received: April 16, 2017
Revised: November 23, 2017
Accepted: November 24, 2017
Published: December 21, 2017

REFERENCES

Aiken, A., and Khokha, R. (2010). Unraveling metalloproteinase function in skeletal biology and disease using genetically altered mice. Biochim. Biophys. Acta *1803*, 121–132.

Al-Nuaimi, Y., Hardman, J.A., Biro, T., Haslam, I.S., Philpott, M.P., Toth, B.I., Farjo, N., Farjo, B., Baier, G., Watson, R.E.B., et al. (2014). A meeting of two chronobiological systems: circadian proteins Period1 and BMAL1 modulate the human hair cycle clock. J. Invest. Dermatol. *134*, 610–619.

de Almeida Prado, D.G., Filho, H.N., Berretin-Felix, G., and Brasolotto, A.G. (2015). Speech articulatory characteristics of individuals with dentofacial deformity. J. Craniofac. Surg. *26*, 1835–1839.

Bailey, S.M., Udoh, U.S., and Young, M.E. (2014). Circadian regulation of metabolism. J. Endocrinol. *222*, R75–R96.

Basner, M., Babisch, W., Davis, A., Brink, M., Clark, C., Janssen, S., and Stansfeld, S. (2014). Auditory and non-auditory effects of noise on health. Lancet *383*, 1325–1332.

Bass, J., and Takahashi, J.S. (2010). Circadian integration of metabolism and energetics. Science *330*, 1349–1354.

Bedrosian, T.A., and Nelson, R.J. (2013). Influence of the modern light environment on mood. Mol. Psychiatry *18*, 751–757.

Bejdova, S., Krajicek, V., Veleminska, J., Horak, M., and Velemínský, P. (2013). Changes in the sexual dimorphism of the human mandible during the last 1200 years in central Europe. Homo *64*, 437–453.

Bell-Pedersen, D., Cassone, V.M., Earnest, D.J., Golden, S.S., Hardin, P.E., Thomas, T.L., and Zoran, M.J. (2005). Circadian rhythms from multiple oscillators: lessons from diverse organisms. Nat. Rev. Genet. *6*, 544–556.

Bibbins-Domingo, K., Grossman, D.C., Curry, S.J., Davidson, K.W., Epling, J.W., Jr., Garcia, F.A., Herzstein, J., Kemper, A.R., Krist, A.H., Kurth, A.E., et al. (2017). Screening for obstructive sleep apnea in adults: US Preventive Services Task Force recommendation statement. JAMA *317*, 407–414.

Boell, L., and Tautz, D. (2011). Micro-evolutionary divergence patterns of mandible shapes in wild house mouse (*Mus musculus*) populations. BMC Evol. Biol. *11*, 306.

Bunger, M.K., Wilsbacher, L.D., Moran, S.M., Clendenin, C., Radcliffe, L.A., Hogenesch, J.B., Simon, M.C., Takahashi, J.S., and Bradfield, C.A. (2000). Mop3 is an essential component of the master circadian pacemaker in mammals. Cell *103*, 1009–1017.

Chai, Y., and Maxson, R.E., Jr. (2006). Recent advances in craniofacial morphogenesis. Dev. Dyn. *235*, 2353–2375.

Curtis, A.M., Fagundes, C.T., Yang, G., Palsson-McDermott, E.M., Wochal, P., McGettrick, A.F., Foley, N.H., Early, J.O., Chen, L., Zhang, H., et al. (2015). Circadian control of innate immunity in macrophages by miR-155 targeting Bmal1. Proc. Natl. Acad. Sci. USA *112*, 7231–7236.

Dibner, C., and Schibler, U. (2015). Circadian timing of metabolism in animal models and humans. J. Intern. Med. *277*, 513–527.

Dudek, M., and Meng, Q.J. (2014). Running on time: the role of circadian clocks in the musculoskeletal system. Biochem. J. *463*, 1–8.

Dudek, M., Gossan, N., Yang, N., Im, H.J., Ruckshanthi, J.P., Yoshitane, H., Li, X., Jin, D., Wang, P., Boudiffa, M., et al. (2016). The chondrocyte clock gene Bmal1 controls cartilage homeostasis and integrity. J. Clin. Invest. *126*, 365–376.

Eguchi, T., Kubota, S., Kawata, K., Mukudai, Y., Uehara, J., Ohgawara, T., Ibaragi, S., Sasaki, A., Kuboki, T., and Takigawa, M. (2008). Novel transcription-factor-like function of human matrix metalloproteinase 3 regulating the CTGF/CCN2 gene. Mol. Cell. Biol. *28*, 2391–2413.

Flores-Pliego, A., Espejel-Nunez, A., Castillo-Castrejon, M., Meraz-Cruz, N., Beltran-Montoya, J., Zaga-Clavellina, V., Nava-Salazar, S., Sanchez-Martinez, M., Vadillo-Ortega, F., and Estrada-Gutierrez, G. (2015). Matrix metalloproteinase-3 (MMP-3) is an endogenous activator of the MMP-9 secreted by placental leukocytes: implication in human labor. PLoS One *10*, e0145366.

Franco, G.C., Kajiya, M., Nakanishi, T., Ohta, K., Rosalen, P.L., Groppo, F.C., Ernst, C.W., Boyesen, J.L., Bartlett, J.D., Stashenko, P., et al. (2011). Inhibition of matrix metalloproteinase-9 activity by doxycycline ameliorates RANK ligand-induced osteoclast differentiation in vitro and in vivo. Exp. Cell Res. *317*, 1454–1464.

Fu, L., Patel, M.S., Bradley, A., Wagner, E.F., and Karsenty, G. (2005). The molecular clock mediates leptin-regulated bone formation. Cell *122*, 803–815.

Gafni, Y., Ptitsyn, A.A., Zilberman, Y., Pelled, G., Gimble, J.M., and Gazit, D. (2009). Circadian rhythm of osteocalcin in the maxillomandibular complex. J. Dental Res. *88*, 45–50.

Garcia, A.J., Tom, C., Guemes, M., Polanco, G., Mayorga, M.E., Wend, K., Miranda-Carboni, G.A., and Krum, S.A. (2013). ERalpha signaling regulates MMP3 expression to induce FasL cleavage and osteoclast apoptosis. J. Bone Miner. Res. *28*, 283–290.

Gerhart-Hines, Z., and Lazar, M.A. (2015). Circadian metabolism in the light of evolution. Endocr. Rev. *36*, 289–304.

Gottlieb, D.J., Yenokyan, G., Newman, A.B., O'Connor, G.T., Punjabi, N.M., Quan, S.F., Redline, S., Resnick, H.E., Tong, E.K., Diener-West, M., et al. (2010). Prospective study of obstructive sleep apnea and incident coronary heart disease and heart failure: the Sleep Heart Health Study. Circulation *122*, 352–360.

Hamid, W., and Asad, S. (2003). Prevalence of skeletal components of malocclusion using composite cephalometric analysis. Pak. Oral Dental J. *23*, 137–144.

Holmbeck, K., Bianco, P., Pidoux, I., Inoue, S., Billinghurst, R.C., Wu, W., Chrysovergis, K., Yamada, S., Birkedal-Hansen, H., and Poole, A.R. (2004). The metalloproteinase MT1-MMP is required

for normal development and maintenance of osteocyte processes in bone. J. Cell Sci. *118* (Pt 1), 147–156.

Huang, N., Chelliah, Y., Shan, Y., Taylor, C.A., Yoo, S.H., Partch, C., Green, C.B., Zhang, H., and Takahashi, J.S. (2012). Crystal structure of the heterodimeric CLOCK: BMAL1 transcriptional activator complex. Science *337*, 189–194.

Huja, S.S., Fernandez, S.A., Hill, K.J., and Li, Y. (2006). Remodeling dynamics in the alveolar process in skeletally mature dogs. Anat. Rec. A Discov. Mol. Cell. Evol. Biol. *288*, 1243–1249.

Jensen, L.D., Cao, Z., Nakamura, M., Yang, Y., Brautigam, L., Andersson, P., Zhang, Y., Wahlberg, E., Lanne, T., Hosaka, K., et al. (2012). Opposing effects of circadian clock genes bmal1 and period2 in regulation of VEGF-dependent angiogenesis in developing zebrafish. Cell Rep. *2*, 231–241.

Kaneshi, Y., Ohta, H., Morioka, K., Hayasaka, I., Uzuki, Y., Akimoto, T., Moriichi, A., Nakagawa, M., Oishi, Y., Wakamatsu, H., et al. (2016). Influence of light exposure at nighttime on sleep development and body growth of preterm infants. Sci. Rep. *6*, 21680.

Kendzerska, T., Gershon, A.S., Hawker, G., Tomlinson, G., and Leung, R.S. (2014). Obstructive sleep apnea and incident diabetes. A historical cohort study. Am. J. Respir. Crit. Care Med. *190*, 218–225.

Kohyama, J. (2014). The possible long-term effects of early-life circadian rhythm disturbance on social behavior. Expert Rev. Neurother. *14*, 745–755.

Landgraf, D., Tsang, A.H., Leliavski, A., Koch, C.E., Barclay, J.L., Drucker, D.J., and Oster, H. (2015). Oxyntomodulin regulates resetting of the liver circadian clock by food. Elife *4*, e06253.

Li, D., Weber, D.R., Deardorff, M.A., Hakonarson, H., and Levine, M.A. (2015a). Exome sequencing reveals a nonsense mutation in MMP13 as a new cause of autosomal recessive metaphyseal anadysplasia. Eur. J. Hum. Genet. *23*, 264–266.

Li, H., Li, T., Fan, J., Li, T., Fan, L., Wang, S., Weng, X., Han, Q., and Zhao, R.C. (2015b). miR-216a rescues dexamethasone suppression of osteogenesis, promotes osteoblast differentiation and enhances bone formation, by regulating c-Cbl-mediated PI3K/AKT pathway. Cell Death Differ. *22*, 1935–1945.

Li, Y., Ge, C., and Franceschi, R.T. (2017). MAP kinase-dependent RUNX2 phosphorylation is necessary for epigenetic modification of chromatin during osteoblast differentiation. J. Cell. Physiol. *232*, 2427–2435.

Lipton, J.O., Yuan, E.D., Boyle, L.M., Ebrahimi-Fakhari, D., Kwiatkowski, E., Nathan, A., Guttler, T., Davis, F., Asara, J.M., and Sahin, M. (2015). The circadian protein BMAL1 regulates translation in response to S6K1-mediated phosphorylation. Cell *161*, 1138–1151.

Lou, J., Wang, Y., Zhang, Z., and Qiu, W. (2017). Activation of MMPs in macrophages by *Mycobacterium tuberculosis* via the miR-223-BMAL1 signaling pathway. J. Cell. Biochem. *118*, 4804–4812.

Maeda, A., Soejima, K., Ogura, M., Ohmure, H., Sugihara, K., and Miyawaki, S. (2008). Orthodontic treatment combined with mandibular distraction osteogenesis and changes in stomatognathic function. Angle Orthod. *78*, 1125–1132.

Marcheva, B., Ramsey, K.M., Buhr, E.D., Kobayashi, Y., Su, H., Ko, C.H., Ivanova, G., Omura, C., Mo, S., Vitaterna, M.H., et al. (2010). Disruption of the clock components CLOCK and BMAL1 leads to hypoinsulinaemia and diabetes. Nature *466*, 627–631.

Maronde, E., Schilling, A.F., Seitz, S., Schinke, T., Schmutz, I., van der Horst, G., Amling, M., and Albrecht, U. (2010). The clock genes Period 2 and Cryptochrome 2 differentially balance bone formation. PLoS One *5*, e11527.

McElderry, J.D., Zhao, G., Khmaladze, A., Wilson, C.G., Franceschi, R.T., and Morris, M.D. (2013). Tracking circadian rhythms of bone mineral deposition in murine calvarial organ cultures. J. Bone Miner. Res. *28*, 1846–1854.

Min, H.Y., Kim, K.M., Wee, G., Kim, E.J., and Jang, W.G. (2016). Bmal1 induces osteoblast differentiation via regulation of BMP2 expression in MC3T3-E1 cells. Life Sci. *162*, 41–46.

Muller, J.E., and Tofler, G.H. (1991). Circadian variation and cardiovascular disease. N. Engl. J. Med. *325*, 1038–1039.

Munzel, T., Gori, T., Babisch, W., and Basner, M. (2014). Cardiovascular effects of environmental noise exposure. Eur. Heart J. *35*, 829–836.

Panda, S., Hogenesch, J.B., and Kay, S.A. (2002). Circadian rhythms from flies to human. Nature *417*, 329–335.

Parry, B.L., Meliska, C.J., Sorenson, D.L., Lopez, A.M., Martinez, L.F., Nowakowski, S., Elliott, J.A., Hauger, R.L., and Kripke, D.F. (2008). Plasma melatonin circadian rhythm disturbances during pregnancy and postpartum in depressed women and women with personal or family histories of depression. Am. J. Psychiatry *165*, 1551–1558.

Peek, C.B., Levine, D.C., Cedernaes, J., Taguchi, A., Kobayashi, Y., Tsai, S.J., Bonar, N.A., McNulty, M.R., Ramsey, K.M., and Bass, J. (2017). Circadian clock interaction with HIF1alpha mediates oxygenic metabolism and anaerobic glycolysis in skeletal muscle. Cell Metab. *25*, 86–92.

Peppard, P.E., Szklo-Coxe, M., Hla, K.M., and Young, T. (2006). Longitudinal association of sleep-related breathing disorder and depression. Arch. Intern. Med. *166*, 1709–1715.

Perkins, N.D. (2006). Post-translational modifications regulating the activity and function of the nuclear factor kappa B pathway. Oncogene *25*, 6717–6730.

Potocki, L., Glaze, D., Tan, D.X., Park, S.S., Kashork, C.D., Shaffer, L.G., Reiter, R.J., and Lupski, J.R. (2000). Circadian rhythm abnormalities of melatonin in Smith-Magenis syndrome. J. Med. Genet. *37*, 428–433.

Powell, W.T., and LaSalle, J.M. (2015). Epigenetic mechanisms in diurnal cycles of metabolism and neurodevelopment. Hum. Mol. Genet. *24*, R1–R9.

Samsa, W.E., Vasanji, A., Midura, R.J., and Kondratov, R.V. (2016). Deficiency of circadian clock protein BMAL1 in mice results in a low bone mass phenotype. Bone *84*, 194–203.

Souslova, V., Townsend, P.A., Mann, J., van der Loos, C.M., Motterle, A., D'Acquisto, F., Mann, D.A., and Ye, S. (2010). Allele-specific regulation of matrix metalloproteinase-3 gene by transcription factor NFkappaB. PLoS One *5*, e9902.

Spengler, M.L., Kuropatwinski, K.K., Comas, M., Gasparian, A.V., Fedtsova, N., Gleiberman, A.S., Gitlin, I.I., Artemicheva, N.M., Deluca, K.A., Gudkov, A.V., et al. (2012). Core circadian protein

CLOCK is a positive regulator of NF-kappaB-mediated transcription. Proc. Natl. Acad. Sci. USA *109*, E2457–E2465.

Van den Steen, P.E., Dubois, B., Nelissen, I., Rudd, P.M., Dwek, R.A., and Opdenakker, G. (2002). Biochemistry and molecular biology of gelatinase B or matrix metalloproteinase-9 (MMP-9). Crit. Rev. Biochem. Mol. Biol. *37*, 375–536.

Steenport, M., Khan, K.M., Du, B., Barnhard, S.E., Dannenberg, A.J., and Falcone, D.J. (2009). Matrix metalloproteinase (MMP)-1 and MMP-3 induce macrophage MMP-9: evidence for the role of TNF-alpha and cyclooxygenase-2. J. Immunol. *183*, 8119–8127.

Stokes, K., Cooke, A., Chang, H., Weaver, D.R., Breault, D.T., and Karpowicz, P. (2017). The circadian clock gene BMAL1 coordinates intestinal regeneration. Cell Mol. Gastroenterol. Hepatol. *4*, 95–114.

Sundaram, K., Nishimura, R., Senn, J., Youssef, R.F., London, S.D., and Reddy, S.V. (2007). RANK ligand signaling modulates the matrix metalloproteinase-9 gene expression during osteoclast differentiation. Exp. Cell Res. *313*, 168–178.

Takarada, T., Kodama, A., Hotta, S., Mieda, M., Shimba, S., Hinoi, E., and Yoneda, Y. (2012). Clock genes influence gene expression in growth plate and endochondral ossification in mice. J. Biol. Chem. *287*, 36081–36095.

Tamemoto, H. (2012). [Circadian rhythm and diabetes]. Nihon Rinsho *70* (*Suppl 5*), 643–647.

Tang, Q., Cheng, B., Xie, M., Chen, Y., Zhao, J., Zhou, X., and Chen, L. (2017). Circadian clock gene bmal1 inhibits tumorigenesis and increases paclitaxel sensitivity in tongue squamous cell carcinoma. Cancer Res. *77*, 532–544.

Wyse, C.A., Biello, S.M., and Gill, J.M. (2014). The bright-nights and dim-days of the urban photoperiod: implications for circadian rhythmicity, metabolism and obesity. Ann. Med. *46*, 253–263.

Xu, C., Ochi, H., Fukuda, T., Sato, S., Sunamura, S., Takarada, T., Hinoi, E., Okawa, A., and Takeda, S. (2016a). Circadian clock regulates bone resorption in mice. J. Bone Miner. Res. *31*, 1344–1355.

Xu, J., Li, Y., Wang, Y., Xu, Y., and Zhou, C. (2016b). Loss of Bmal1 decreases oocyte fertilization, early embryo development and implantation potential in female mice. Zygote *24*, 760–767.

Yaggi, H.K., Concato, J., Kernan, W.N., Lichtman, J.H., Brass, L.M., and Mohsenin, V. (2005). Obstructive sleep apnea as a risk factor for stroke and death. N. Engl. J. Med. *353*, 2034–2041.

Yang, G., Chen, L., Grant, G.R., Paschos, G., Song, W.L., Musiek, E.S., Lee, V., McLoughlin, S.C., Grosser, T., Cotsarelis, G., et al. (2016). Timing of expression of the core clock gene Bmal1 influences its effects on aging and survival. Sci. Transl. Med. *8*, 324ra16.

Zhang, J., Liu, J., Zhu, K., Hong, Y., Sun, Y., Zhao, X., Du, Y., and Chen, Z.J. (2016). Effects of BMAL1-SIRT1-positive cycle on estrogen synthesis in human ovarian granulosa cells: an implicative role of BMAL1 in PCOS. Endocrine *53*, 574–584.

Zheng, L., Seon, Y.J., Mourao, M.A., Schnell, S., Kim, D., Harada, H., Papagerakis, S., and Papagerakis, P. (2013). Circadian rhythms regulate amelogenesis. Bone *55*, 158–165.